Quasiparticle band structure and optical spectrum of LiF(001)

Neng-Ping Wang,* Michael Rohlfing, Peter Krüger, and Johannes Pollmann
Institut für Festkörpertheorie, Universität Münster, Wilhelm-Klemm-Straße 10, D-48149 Münster, Germany
(Received 12 August 2002; revised manuscript received 12 November 2002; published 19 March 2003)

We present the quasiparticle band structure and the optical excitation spectrum of bulk LiF and the LiF(001)-(1×1) surface. First, we calculate the ground-state geometry of the bulk and the surface using density-functional theory within the local-density approximation. Next, applying the *GW* approximation for the self-energy, we evaluate the corresponding quasiparticle band structure. Finally, we calculate the electron-hole interaction, solve the Bethe-Salpeter equation for the two-particle Green function, and investigate the optical-absorption spectrum. The obtained spectrum of bulk LiF, which is dominated by a strong exciton peak at 12.7 eV, is in good agreement with experiment. At the LiF(001)-(1×1) surface, the excitonic effects are strongly modified with respect to the bulk. In particular, we observe a surface exciton at 12.3 eV, i.e., 0.4 eV below the bulk exciton.

DOI: 10.1103/PhysRevB.67.115111 PACS number(s): 78.20.Bh, 71.35.Cc, 73.20.At, 78.66.Nk

I. INTRODUCTION

Optical spectra play a central role in materials science. Absorption, reflectivity, photoluminescence, and other spectroscopic techniques are widely used to characterize materials. In addition, excited states provide the basis for a wide range of technical applications, such as light-emitting devices, solid-state lasers, optical fibers, and photochemical and photobiological reactions. In the case of surfaces, spectra are important tools to identify the surface structure[1] and to monitor processes like molecular adsorption, catalysis, and chemical reactions.[2]

The alkali halides can be considered as prototype insulator materials since they allow us to carefully investigate the role of electronic correlation on the boundary between localized and delocalized electronic states. They are important materials for a range of optical applications; in addition, they show a variety of interesting interaction mechanisms between the electronic and geometric structure. Many of these features, like the characterization of color centers or the emission of atoms from laser-excited alkali halides, involve excited electronic states. Among the alkali halides, LiF takes an extreme position, having the largest fundamental bulk band gap (14.4 eV) and showing an exciton peak at 12.6 eV. It is the ideal material to study excited electronic states, the formation of excitons, and the corresponding optical properties.

Excited states of surface systems usually differ qualitatively from those of bulk systems in many respects. In many cases, characteristic surface states are observed both in the band structure and in the optical spectrum of materials. These states, that are strongly localized at the surface, are important for the characterization of the surface, and they are very interesting since they allow us to study electronic interaction effects on an extremely short length scale (a few Å). In the present work we focus on excited electronic states at the LiF(001) surface, in particular on the surface exciton, which has a binding energy larger than the LiF bulk exciton.

The LiF(001) surface exciton has been investigated extensively,[3–7] but no final conclusion regarding its nature could be drawn, so far. In electron energy-loss spectroscopy (EELS) on LiF(001),[3,4] transitions have been observed at energies of about 10.3 eV, which would be more than 2 eV below the bulk exciton. In excitation-stimulated particle desorption from LiF,[5] the onset of desorption has been observed at an excitation energy of 9.6 eV, which was interpreted as the surface exciton. In a theoretical study,[6] based on quantum-chemical approaches and a cluster geometry, a surface exciton energy of 11.5 eV has been reported. The data scatter over a broad range of excitation energies; moreover, the reported difference of more than 2 eV between the excitation energy of the surface exciton and the bulk exciton appears to be very large for an ionic material, in which already the bulk excitons are rather Frenkel-like, having an exciton radius of a few Å, only. The purpose of our present work is to analyze the formation of the exciton in detail and to contribute to the interpretation of the available data.

The theoretical description of the excited states of surfaces poses several demanding problems. The electronic structure of surface systems is dominated by quantum states localized on a length scale of only a few Å, calling for an atomic-scale approach. In addition, optical spectra are severely influenced by electronic many-body effects. To account for both, we employ a highly reliable *ab initio* scheme of many-body perturbation theory,[8–13] based on density-functional theory for the electronic ground state.

Density-functional theory in the local-density approximation (LDA) has proven to be a very powerful tool for the calculation of the electronic ground-state properties of many materials. Spectral properties, on the other hand, are in general not directly accessible in such a calculation since DFT does not describe excited electronic states, like quasiparticle (QP) excitations and correlated electron-hole excitations. The state-of-the-art approach to calculate QP spectra is Hedin's *GW* approximation (*GWA*),[14,15] in which the nonlocal, energy-dependent electron self-energy operator is approximated by a convolution of the one-electron Green function and the dynamically screened Couloumb interaction. Very accurate quasiparticle properties have been obtained by this method.[8]

Optical spectra of nonconducting solids are dominated by electron-hole correlation effects that are described neither by

 ©2003 The American Physical Society

DFT nor by *GWA*. It has been shown that the investigation of optical excitations requires an effective two-body approach, which must take the electron-hole interaction into consideration,[9–13] thus going beyond the independent-quasiparticle picture. A rigorous approach to optical spectra is given by evaluating the two-body Green function.[16] The equation of motion for the two-body Green function (the Bethe-Salpeter equation) is solved, yielding coupled excited electron-hole states. Using the optical transition matrix elements corresponding to these coupled electron-hole excitation states (which are expressed as coherent superpositions of the matrix elements of free electron-hole pairs), the entire linear optical spectrum of a material can be obtained. This approach has been applied successfully to investigate semiconductors and insulators.[10–13] Up to date, most of these calculations were focused on bulk crystals. A few studies on semiconductor *surfaces* have been presented,[12,17–19] indicating very pronounced electron-hole correlation effects. In this paper, we present an *ab initio* calculation of the optical response of an *insulator* surface, i.e., of LiF(001)-(1×1). We discuss the excitonic effects on the absorption and reflectivity spectra of the surface in some detail.

The paper is organized as follows. In Sec. II, we briefly summarize the basic theoretic formulation. In Sec. III, we discuss the LiF bulk crystal. In Sec. IV, we determine the ground-state geometry of the LiF(001)-(1×1) surface and discuss the LDA and GWA band structures of the surface. In Sec. V, our results for the optical absorption and reflectivity spectrum of the surface are presented. Finally, a short summary is given in Sec. VI.

II. BASIC THEORETICAL FORMULATION

A. Ground state

The ground-state properties of semiconductors and insulators can be obtained from density-functional theory (DFT) in the local-density approximation (LDA), yielding LDA band-structure energies, wave functions, and the total energy. Based on the total energy and the resulting forces on the atoms, we optimize the geometric structure of the bulk and of the surface by relaxing the system to mechanical equilibrium.

Gaussian orbitals are used to construct the LDA basis sets.[20] We use 30 Gaussian orbitals of *s*, *p*, *d*, and *s** type for both Li and F. The decay constants (in atomic units) are 0.3, 1.34, and 6.0 for Li and 0.2, 0.95, and 4.5 for F. The same basis functions are also used for the representation of all quantities occurring in the *GW* self-energy operator and the electron-hole interaction in the next section.

For the ionic potential we use nonlocal, norm-conserving *ab initio* pseudopotentials. The potential for F is taken from Ref. 21. We find that the Li 1*s* state (which is often treated as a core state and eliminated by pseudopotential construction) significantly influences the structural properties of LiF. To account for this, in particular for the following surface calculations, we include the Li 1*s* state among the valence states.

B. Quasiparticle band structure

Quasiparticle excitations can be described using many-body perturbation theory,[14,15] in which the self-energy operator Σ is expanded in a series containing the one-body Green function G_1 and the screened Coulomb interaction W of the system. The first term of the expansion constitutes the *GW* approximation:[15,20,22]

$$\Sigma(\mathbf{r},\mathbf{r}',E)=\frac{i}{2\pi}\int e^{-i\omega 0^+}G_1(\mathbf{r},\mathbf{r}',E-\omega)W(\mathbf{r},\mathbf{r}',\omega)d\omega. \tag{1}$$

In practical evaluations, the one-body Green function G_1 is described approximately in terms of the results of the DFT-LDA calculation. For the frequency dependence of W we employ a generalized plasmon-pole approximation. The static part $W(\omega=0)$ of the interaction is calculated using either the random-phase approximation (RPA) or a model dielectric function.[22] After constructing the self-energy operator Σ, we solve the quasiparticle equation.[20] In most cases, the LDA wave functions ψ_n^{LDA} are already very close to ψ_n^{QP}. Therefore, the QP equation can often be solved perturbatively, leading to

$$E_n^{QP}=E_n^{LDA}+\langle\psi_n^{LDA}|\Sigma(E_n^{QP})-V_{xc}|\psi_n^{LDA}\rangle \tag{2}$$

which, as we have carefully investigated, is sufficient in our present case. The expectation value of $[\Sigma(E_n^{QP})-V_{xc}]$ defines a QP correction to the LDA band structure. For semiconductors and insulators, this correction is often in the order of 1–10 eV.

C. Optical excitation

While the *GWA* yields band structures in good agreement with experimental data for single-particle excitations, optical properties cannot be obtained correctly from QP band structures within an independent-particle picture. This is due to the interaction between the excited electrons and holes occurring in optical excitations. To describe the resulting two-body correlation effects on optical properties, an effective two-particle theory is required. The most general procedure for calculating optical spectra is to consider the two-body Green function G_2 (or, equivalently, the corresponding electron-hole correlation function) and to solve the equation of motion for it.[16] This procedure can be formulated in terms of coupled electron-hole excited states $|S_\mathbf{Q}\rangle$. We assume that these states can be expanded in a basis given by the QP states as[13]

$$\begin{aligned}|S_\mathbf{Q}\rangle&=\sum_\mathbf{k}\sum_v^{hole}\sum_c^{elec}A_{vc\mathbf{k}}^{S\mathbf{Q}}|vc\mathbf{k}\rangle\\&=\sum_\mathbf{k}\sum_v^{hole}\sum_c^{elec}A_{vc\mathbf{k}}^{S\mathbf{Q}}\hat{a}_{v\mathbf{k}}^\dagger\hat{b}_{c,\mathbf{k}+\mathbf{Q}}^\dagger|0\rangle,\end{aligned} \tag{3}$$

where $\hat{a}_{v\mathbf{k}}^\dagger$ and $\hat{b}_{c,\mathbf{k}+\mathbf{Q}}^\dagger$ denote the operators creating a hole (in valence band v at wave vector $\mathbf{k}$) and an electron (in conduction band c at wave vector $\mathbf{k}+\mathbf{Q}$), respectively, in the many-body ground state $|0\rangle$. $\mathbf{Q}$ is the total momentum of the

electron-hole state which, in optical processes, corresponds to the momentum of the involved photon. Since the photon wavelength is very large compared to the lattice constant of crystals, the momentum **Q** of the exciton created in photoabsorption is very close to zero. Nevertheless, the direction of the exciton momentum **Q** may be important for details of the spectrum. For simplicity of the equations, we suppress the index **Q** at $|S\rangle$ in the following.

Since the electronic ground state of LiF is given by a closed-shell spin-singlet state, the excitations can be classified (in the absence of spin-orbit interaction) as singlet-to-singlet and singlet-to-triplet excitations. We will focus on the singlet-to-singlet transitions that are relevant for the optical spectra. From the equation of motion of G_2, one obtains the following equation of motion of the excited states $|S\rangle$ (usually called the Bethe-Salpeter equation, BSE):[13,16]

$$(E^{QP}_{c,\mathbf{k}+\mathbf{Q}}-E^{QP}_{v,\mathbf{k}})A^S_{vc\mathbf{k}}+\sum_{\mathbf{k}'}\sum_{v'}^{hole}\sum_{c'}^{elec}\langle vc\mathbf{k}|K^{eh}|v'c'\mathbf{k}'\rangle A^S_{v'c'\mathbf{k}'} = \Omega_S A^S_{vc\mathbf{k}}. \quad (4)$$

The electron-hole interaction K^{eh} consists of a screened, direct term $K^{eh,d}$ and an exchange term $K^{eh,x}$. In general, $K^{eh,d}$ is frequency dependent. For the system under study, however, the exciton *binding energy* is small in comparison to the band gap, which defines the characteristic energy scale of the dielectric screening. Therefore a statically screened electron-hole interaction can be used (for details, see Refs. 13 and 16).

Once the Bethe-Salpeter equation (4) is solved, the obtained coefficients $A^S_{vc\mathbf{k}}$ can be used to evaluate the real-space wave function of an excited state $|S\rangle$,

$$\chi_S(\mathbf{r_h},\mathbf{r_e})=\sum_{\mathbf{k}}\sum_{v}^{hole}\sum_{c}^{elec} A^S_{vc\mathbf{k}}\psi^*_{v\mathbf{k}}(\mathbf{r_h})\psi_{c\mathbf{k}+\mathbf{Q}}(\mathbf{r_e}). \quad (5)$$

Here, $\mathbf{r_e}$ and $\mathbf{r_h}$ denote the coordinates of the electron and the hole, respectively. Furthermore, the entirety of all excited states yields the optical spectrum (see, e.g., Ref. 13). Before we address the main topic of our work, i.e., the optical excitations of LiF(001)-(1×1), we briefly summarize the spectral properties of the bulk, as well as the geometric and electronic properties of the surface.

III. LiF BULK CRYSTAL

We first address the bulk crystal of LiF to check the validity of our approach and to provide a basis for discussing the surface features of LiF(001)-(1×1) in the next section.

LiF is an ionic insulator material, having rocksalt structure with a lattice constant of $a=4.026$ Å. By LDA total-energy minimization we obtain a slightly lower theoretical lattice constant of $a=3.918$ Å. The band gap is highly sensitive to the lattice constant: when a is reduced from the experimental to the theoretical value, the fundamental LDA energy gap increases from 8.26 to 8.91 eV, while the dispersion of the bands remains unchanged. Note that the electron-hole interaction effects depend mainly on the band dispersion, not on the fundamental gap. Since the band dispersion is not affected by such small changes of the lattice constant, the main effect of a change in the lattice constant on the optical spectra is a rigid shift of the entire spectrum in energy. We consider the band structure at the experimental lattice constant as the more realistic electronic quasiparticle spectrum. Therefore we calculate the spectral properties at the experimental lattice constant.

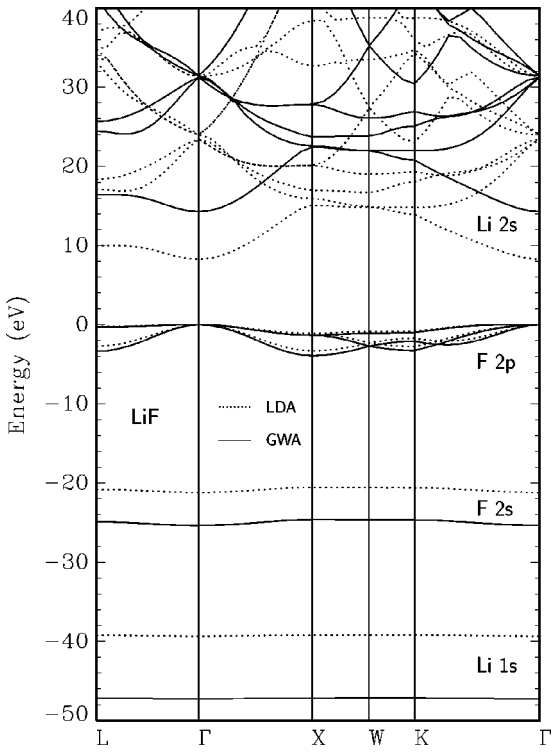

FIG. 1. Bulk band structure of LiF, as obtained within GWA (solid curve) and within LDA (dotted curve).

Figure 1 shows the LiF bulk band structure, calculated within GWA (solid lines). For comparison sake the LDA band structure (dashed lines) is shown, as well. The *GW* valence-band structure consists of five bands, that can unambiguously be classified as a Li 1*s* band (at −47.2 eV), a F 2*s* band (at −24.8 eV), and three F 2*p* bands (between −3.9 and 0 eV). Our calculated F 2*p* band width is in excellent agreement with the measured band width of 3.5 eV,[23] and a previous theoretical result of 3.6 eV.[24] We will often label the lowest conduction band (having its minimum at the Γ point) as the Li 2*s* band, although this classification is not exactly possible due to significant coupling of the Li 2*s* orbital to other states. The fundamental band gap amounts to 8.3 eV, only, in LDA. Due to the QP corrections, it is increased by about 6 eV, resulting in a QP gap of 14.3 eV. Such large GWA corrections are expected in a system in which the dielectric screening is weak. In addition to the change of the gap, also the dispersion of the bands is affected by the QP corrections, leading to slightly increased band widths of the F 2*p* bands and of the lowest conduction band. The F 2*s* and Li 1*s* core levels observe much stronger QP corrections of −4.2 and −7.9 eV, respectively, which is typical for strongly localized electronic states. The Li 1*s* and F 2*s* core levels have been observed experimentally by Johansson *et al.*[25] at

energies of −49.8 and −23.9 eV, respectively. Kowalczyk *et al.* have reported a core-level energy of −24.9 eV for F $2s$.[26] Our *GW* energies of these two core levels within RPA are close to these experimental data. Clearly, *GW* corrections to the LDA improve the agreement with experiment.

The screening in the above *GW* calculation has been treated within RPA, which is numerically very demanding, in particular for the surface system to be addressed in the next section. For the surface calculations, it would be highly desirable therefore to replace the RPA dielectric function by a model dielectric function like the one suggested by Hybertsen and Louie.[22] This model function has been shown to describe the dielectric function of bulk and surface systems very accurately, leading to very reliable QP band-structure energies within the *GWA*.[20] [We have carried out some test calculations for LiF(001) which indicate that the uncertainty induced by the model function does not exceed about 0.1 eV in the band-structure energies.] In the case of bulk LiF, we find that this model dielectric function (using the same dielectric constant of 1.8 as obtained by the RPA) does indeed yield basically the same *GW* QP band structure as the RPA. For the occupied F $2p$ bands and for the lowest conduction band, the largest deviation between the QP energies resulting from RPA and from the model amounts to 0.06 eV, only. The accuracy of the screening using the model dielectric function is thus sufficient for the following discussion of the optical spectra of the surface, while being numerically much more efficient than RPA. We will therefore employ the model dielectric function throughout the remainder of the paper except where noted. We note in passing that the model dielectric function does not describe accurately the QP energy of the localized Li $1s$ state, which results as −45.8 eV compared to the RPA result of −47.2 eV (see the discussion of the surface core-level shift in Sec. IV). Since such energetically deep states are irrelevant for the optical properties of low-energy excitations, this deviation does not matter for the calculation of the spectra.

Using the approach presented in Sec. IIC, the optical spectrum can be calculated. Initially, we have included the three F $2p$ valence bands (i.e., $v=3-5$) and the four lowest conduction bands (including the Li $2s$ band, i.e., $c=6-9$) in the evaluation of Eq. (4). The low-lying Li $1s$ and F $2s$ bands (i.e., $v=1,2$) need not to be taken into account since they cannot contribute to the excitations below ~25 eV. The latter are in the focus of our interest. We use 256 k points, yielding a spectral resolution of better than ~0.2 eV in the continous part of the resulting spectrum. The electron-hole matrix in Eq. (4) thus has a size of $3\times4\times256=3072$.

After solving the eigenvalue problem of Eq. (4), the optical-absorption spectrum is calculated including in total the seven bands mentioned above. The results are compiled in Fig. 2. The dashed-dotted curve indicates the spectrum without electron-hole interaction effects, thus corresponding to independent interband transitions. The solid curve shows the spectrum with the interaction included. Apparently, significant changes occur due to the interaction, in particular in the low-energy range which is now dominated by a characteristic exciton peak at 12.7 eV, i.e., 1.6 eV below the QP gap. The circles denote experimental data.[27] Clearly, very good agreement between experiment and theory is obtained for both the energy and the oscillator strength (amplitude× width) of the main peak. The results presented here are essentially the same as those discussed in Refs. 11 and 12. They are included at this point to motivate one further simplification of the calculations which provides the basis for the following investigations of the surface.

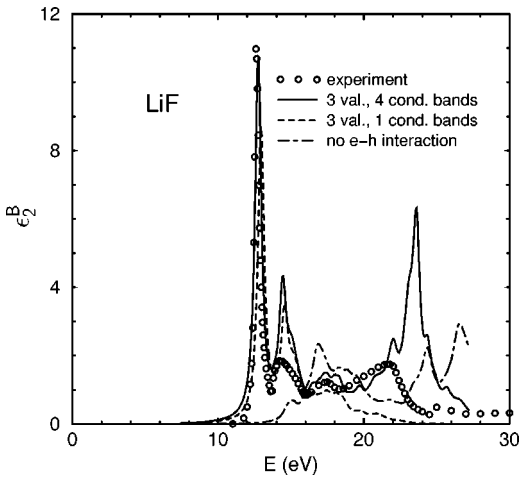

FIG. 2. Calculated optical absorption spectrum $\epsilon_2(\omega)$ of bulk LiF, obtained from two different subsets of occupied and empty bands (see text). The dashed-dotted curve indicates the free interband spectrum, i.e., with the electron-hole interaction switched off. A Lorentzian broadening of 0.3 eV has been used. The open circles denote the optical data measured by Roessler and Walker (Ref. 27).

As just discussed, the use of three valence and four conduction bands allows for the calculation of a converged ϵ_2 spectrum for excitation energies up to ~25 eV. Analysing the influence of the four conduction bands on our results, we have observed that the main contributions stem from the lowest conduction band (Li $2s$ band) while the three higher conduction bands ($c=7-9$) do not contribute significantly to the low-energy part of the spectrum. Therefore we do not need to retain the latter bands in the electron-hole matrix of Eq. (4). It is sufficient to evaluate the optical spectrum from the three F $2p$ valence and the one Li $2s$ conduction bands, only (i.e., by only considering transitions from F $2p$ to Li $2s$). The resulting spectrum for bulk LiF is shown by the dashed line in Fig. 2. Apparently, for energies below 18 eV this spectrum is in good agreement with the above discussed fully converged spectrum. This holds, in particular, for the exciton peak. In the case of the LiF(001) surface this means that, as long as we are mainly interested in the low-energy exciton states—say below 18 eV—it is sufficient to restrict the excitations to transitions from F $2p$ to Li $2s$.

IV. LiF(001)-(1×1) SURFACE BAND STRUCTURE

Now we turn to the LiF(001) surface. We consider the unreconstructed (1×1) surface, which is prototypical for (001) surfaces of rocksalt-structured insulators.[28] The DFT-LDA is used to determine the ground-state geometry. We take the surface normal as the z direction. The surface is represented by a supercell geometry of six atomic layers con-

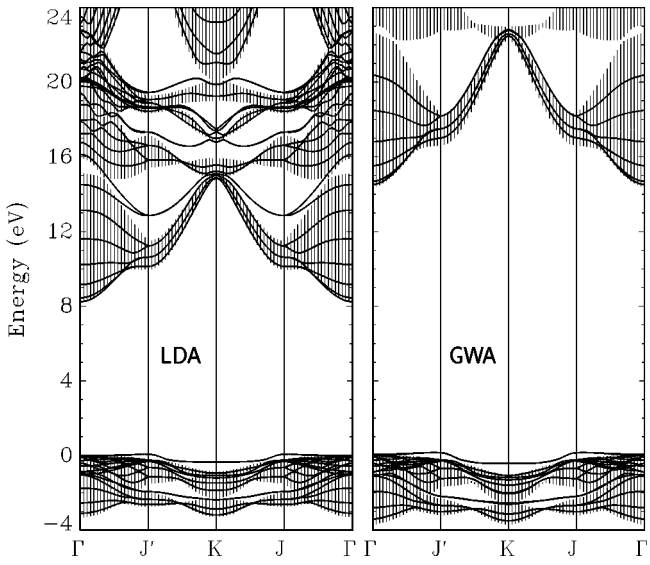

FIG. 3. Surface band structure of LiF(001)-(1×1), obtained within LDA (left panel) and GWA (right panel). The vertical lines indicate the projected bulk band structure. In the right panel, only the bands that are included in the Bethe-Salpeter equation are shown.

taining six Li atoms and six F atoms in the unit cell, resulting in 30 valence bands. For the structure optimization and the calculation of the electronic surface band structure the same basis states as in the bulk calculations are used. The optimized geometry turns out to be close to that of the ideal surface, with very small relaxations, only. In the surface layer, the Li atoms relax towards the substrate by $\delta z = -0.03$ Å while the F atoms relax outwards by $\delta z = 0.03$ Å.[29] These results are in very good agreement with the data of a very recent low-energy electron diffraction measurement[30] showing an inward relaxation of the Li atoms by $\delta z = -0.02$ Å and an outward relaxation of the F atoms by $\delta z = 0.02$ Å.

Figure 3 shows the LDA and *GWA* band structures of the relaxed LiF(001)-(1×1) surface. Most of the states are bulklike, being energetically in resonance with bulk states. Near the Γ point, only the highest valence bands and the lowest conduction bands are truly localized surface states. As expected for an ionic system without chemically active dangling-bond surface states, the QP corrections at the surface are very similar to those in the bulk.

For completeness sake, we also report on the surface properties of the Li 1*s* core state at −47.2 eV (not shown in Fig. 3), in particular on its surface core-level shift (SCLS). The Li 1*s* level at the Li surface atoms is lower in energy than the Li 1*s* level in the bulk. The SCLS amounts to −0.2 eV in LDA and −0.5 eV in GWA. We note in passing that a careful calculation of the QP correction to Li 1*s* and its SCLS is only possible with the RPA dielectric function. The model dielectric function does not correctly describe the related self-energy and the SCLS of this strongly localized state, in contrast to the excellent results of the states close to the gap (see above). We are not aware of experimental data on the Li 1*s* SCLS at the LiF(001) surface.

V. OPTICAL EXCITATIONS OF THE LiF(001)-(1×1) SURFACE

Now we address the calculation of excited states and the optical spectrum of the LiF(001)-(1×1) surface.

A. Introductory remarks

As mentioned above, the surface is represented by a supercell geometry of six atomic layers with six Li and six F atoms per supercell (i.e., six times as many as in the bulk calculation of Sec. III) and sufficiently many vacuum layers to decouple the two surfaces of neighboring supercells. As far as the coupled electron-hole excitations in the slabs of each supercell are concerned, this slab size would imply that six times as many valence and conduction bands have to be taken into account to be consistent with the bulk calculations. The case of three valence and four conduction bands in the bulk calculation of the ϵ_2 spectrum would then translate to 18 valence and 24 conduction bands in the slab representing the surface. Simply speaking, the size of the electron-hole band-to-band product basis scales quadratically with the size of the system. Fortunately, less **k** points are necessary for the surface since only the two-dimensional surface Brillouin zone must be sampled, as compared to the three-dimensional bulk Brillouin zone. In practice, we use up to 64 **k** points for the surface as compared to 256 for the bulk. Nonetheless, the corresponding size of the electron-hole matrix for the surface system [Eq. (4)] would amount to $18\times24\times64=27\,648$, which is too demanding for diagonalization. Fortunately, however, we can reduce the size of the matrix in Eq. (4)—without significant loss of accuracy in that part of the optical spectrum we are interested in (say below 18 eV) — by restricting the excitations to transitions from F 2*p* to Li 2*s*. It is thus sufficient to retain 18 valence and 6 conduction bands for the calculation of the optical spectrum of the LiF(001)-(1×1) surface. This subset of bands of the six-layer slab corresponds to the subset of three valence bands (F 2*p*) and one conduction band (Li 2*s*) in our respective bulk calculation (see Sec. III). With 64 **k** points from the surface Brillouin zone, this yields a matrix size of $18\times6\times64=6912$, which can be handled. Therefore all further discussion will be based on this restricted subset of bands.

B. Electron-hole excited states

Let us first consider the case of normal incidence, i.e., the electric-field vector of the light is oriented in the *xy* plane parallel to the surface. Defining the exciton momentum **Q** along the *z* direction and solving the eigenvalue problem of Eq. (4), the excitation energies Ω_S and coefficients $A^S_{vc\mathbf{k}}$ are obtained. The top panel of Fig. 4 depicts the joint density of states, which is characterized by a number of exciton states. For the light with the electric field polarized along the *x* or *y* directions, the bottom panel of Fig. 4 shows the optical absorption spectrum, which is dominated by two strong peaks below the QP surface band gap ($E^{surf}_{gap}=14.4$ eV). The most important exciton states are also compiled in Table I.

Next we address the excited states and their optical properties in detail. Let us label the first four peaks in the top

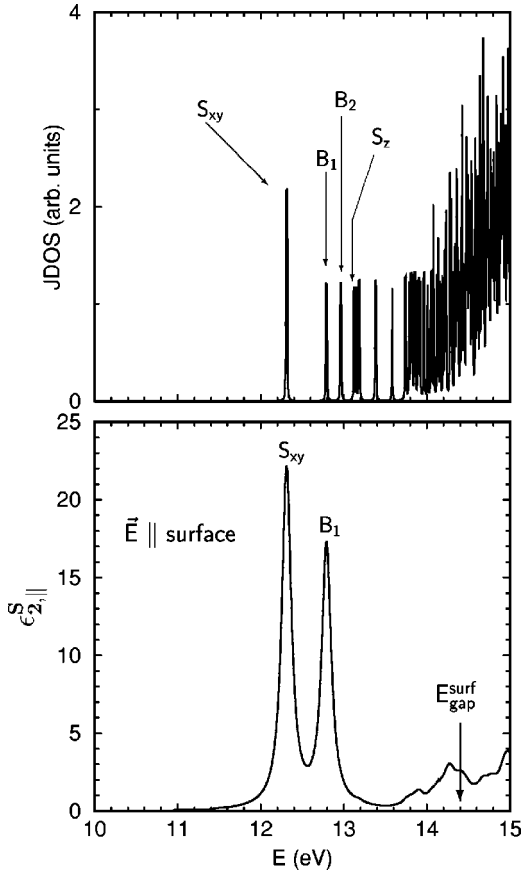

FIG. 4. Top panel: joint density of states (in arbitrary units) of the surface system. Bottom panel: optical-absorption spectrum of the surface calculated for normal incidence of light. The broadening is 0.07 eV.

panel of Fig. 4, in energy-increasing order, as S_{xy} (at 12.3 eV; fourfold degenerate),[31] B_1 (at 12.8 eV; twofold degenerate),[31] B_2 (at 13.0 eV; twofold degenerate),[31] and S_z (at 13.1 eV; twofold degenerate).[31] The analysis of the wave functions of S_{xy} and S_z clearly shows that they are strongly localized at the surface, i.e., these states are surface excitons (see below). The wave functions of B_1 and B_2, on the other hand, reveal that they originate from the LiF bulk excitons, modified by quantum-confinement effects due to the finite thickness of the slab. More bulklike states occur at higher energies, but they become more and more difficult to identify due to increasingly complicated mixture with other states.

TABLE I. Calculated surface exciton states at the LiF(001)-(1×1) surface. The surface is represented by a slab geometry of six atomic layers (see text). The momentum is chosen perpendicular to the surface.

State	Energy [eV]	Degeneracy (Ref. 31)	Transition
S_{xy}	12.3	4	surf. F $2p_{x/y}\rightarrow$Li$2s$
B_1	12.8	2	bulk F $2p_{x/y}\rightarrow$Li$2s$
B_2	13.0	2	bulk F $2p_{x/y}\rightarrow$Li$2s$
S_z	13.1	2	surf. F $2p_z\rightarrow$Li$2s$

Note that the individual bulklike states of our slab are slightly different from those of a semi-infinite LiF crystal. The entirety of all those bulklike states, however, does allow for an excellent representation of the spectral properties of the surface system (see, e.g., the calculation of the reflectivity spectrum in Sec. V). The surface exciton states are unaffected by the finite thickness of the slabs as long as it is large compared to the vertical extent of the surface states (which is only a few Å in the present case).

The binding energy of the lowest exciton S_{xy} is 2.0 eV, which is significantly stronger than the binding energy of the bulk exciton (1.6 eV). S_{xy} thus observes a 25% increase of the electron-hole interaction, as compared to the bulk exciton. Apparently, only the S_{xy} surface state (at 12.3 eV) and the B_1 bulklike state (at 12.8 eV) contribute significantly to the optical response for normal-incidence geometry. This is due to the fact that the states B_2 and S_z have no dipole strength parallel to the surface.

To understand this behavior in more detail, let us discuss the spatial properties of the exciton states. Using the coefficients $A^S_{vc\mathbf{k}}$, the real-space wave function of each exciton state can be evaluated from Eq. (5). $|\chi_S(\mathbf{r}_h,\mathbf{r}_e)|^2$ gives the real-space correlation between the excited hole (at $\mathbf{r}_h$) and electron (at $\mathbf{r}_e$). This quantity is a scalar function in a six-dimensional space $(\mathbf{r}_h,\mathbf{r}_e)$, which makes it difficult to visualize salient features. To analyze the surface-related features of each state, we define a *reduced* correlation function between the z coordinates of the hole and electron by

$$\overline{\chi^2_S}(z_h,z_e) := \int |\chi_S(\mathbf{r}_h,\mathbf{r}_e)|^2 dx_h dy_h dx_e dy_e, \qquad (6)$$

i.e., by averaging the full electron-hole correlation over the coordinates parallel to the surface. $\overline{\chi^2_S}(z_h,z_e)$ gives the averaged distributions of the electron and the hole along the surface normal.

For illustration, the top panel of Fig. 5 shows the contour plot of $\overline{\chi^2_S}(z_h,z_e)$ for a bulk exciton state in the periodic LiF crystal. The horizontal (vertical) axis denotes the z coordinate of the hole (electron). The straight lines indicate the z position of the atomic layers; the spacing corresponds to the interlayer distance of 2.01 Å. The reduced correlation function has its largest amplitude close to the diagonal ($z_h = z_e$), indicating the attractive correlation between hole and electron in the exciton state. For the periodic bulk crystal, the correlation function is periodic in z, corresponding to the free mobility of the exciton as a whole. The fine structure is characterized by a smooth spread of the electron (z_e) over a distance of about $z_h \pm 3$ Å. There is no detailed structure smaller than 3 Å for the electron coordinate because the lowest conduction states in LiF (i.e., Li $2s$) are rather delocalized. For the hole coordinate, on the other hand, there is a strong corrugation, with no amplitude in the regions between the atomic layers. The reason is that the hole results from the F $2p$ orbitals, which are strongly localized on the F atoms. Due to the much larger extent of the envelope function, which ranges from about z_e-3 Å to z_e+3 Å, the hole has

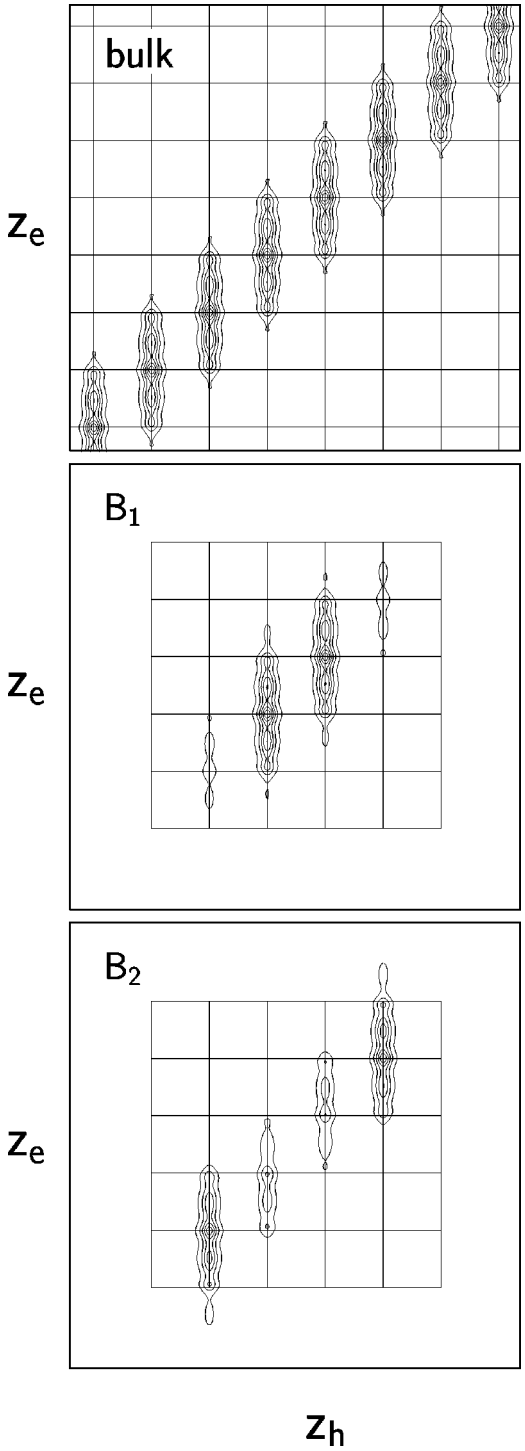

FIG. 5. Reduced z_h/z_e correlation function $\overline{\chi_S^2}$ for the bulk exciton state in bulk LiF (top panel), as well as for the bulklike exciton states B_1 and B_2 of the six-layer slab system (middle and bottom panels). The straight lines indicate the atomic layers (see text).

nonzero amplitude on the neighboring atomic layers. The extent of the hole is thus similar to that of the electron, i.e., $\sim$3 Å in both directions.

The middle and bottom panel of Figs. 5 show the $\overline{\chi_S^2}$ correlation function for the exciton states B_1 and B_2 of our slab calculation. Again, the horizontal and vertical lines indicate the z coordinates of the six atomic layers used in the slab geometry. The correlation function of B_1 has almost zero amplitude at the surface and subsurface layers. Instead, it is localized at the third and fourth layers, i.e., in the center of the slab. The fine structure of the function is essentially the same as that of the bulk exciton discussed in the top panel. The exciton state B_2 behaves in a different way (see the bottom panel). Here the electron and the hole are localized at the second and fifth layers, with very small amplitude at the central layers of the slab. Again, the amplitude at the surface is zero. From these correlation functions we conclude that B_1 and B_2 are bulklike exciton states, with wave functions that are strongly affected by quantum confinement due to the finite slab thickness in the z direction. We interprete B_1 as a bulk exciton with an even envelope function (corresponding to the ground state in a one-dimensional box) while B_2 has an odd envelope function with a node in the center of the slab (corresponding to the second state in a one-dimensional box). Consequently, the excitation energy of B_2 is higher than that of B_1 (0.17 eV), resulting from the higher kinetic energy of the state B_2 with a node. More bulklike states with more complicated nodal structures occur at higher energy.

More detailed information about the states B_1 and B_2 can be obtained from the exciton probability density $|\chi_S(\mathbf{r}_h,\mathbf{r}_e)|^2$ at fixed hole position $\mathbf{r}_h$, showing the distribution of the electron with respect to the hole, or vice versa. The top panel of Fig. 6 shows a side view of this quantity for state B_1, with the hole being fixed at an F atom in one of the two central layers of the slab. The excited electron covers a range of several Å, consistent with the correlation function discussed in Fig. 5. The amplitude of the electron is rather smooth, with maximum values on the central and neighboring F atoms. The simple idea of a Frenkel exciton, with the electron hopping from the F atom to a neighboring Li atom, obviously does not apply in the current system because the corresponding Li $2s$ orbitals are quite delocalized. The bottom panel of Fig. 6 shows the corresponding contour plot of the hole relative to the electron (which is now fixed at the central F atom). This clearly shows that the excited hole consists mainly of F $2p_x/p_y$ orbitals. The same general behavior is found for the exciton state B_2 (not shown here).

The exciton states S_{xy} and S_z behave very differently. This can be seen from their reduced correlation functions $\overline{\chi_S^2}(z_h,z_e)$ shown in the top and bottom panels of Fig. 7. Apparently, both exciton states S_{xy} and S_z are surface states. S_{xy} is completely localized in the outermost atomic layer, with only minimal amplitude of the electron in the subsurface layer. Both particles have significant amplitude in the vacuum region, in particular the electron. In the case of S_z, the electron distribution is similar, while the hole has some amplitude on the subsurface layer, as well. Both states have zero amplitude in the inner layers of the slab, which again indicates that the six-layer slab is sufficiently thick to allow for a converged representation of S_{xy} and S_z.

The top panels of Fig. 8 show the distribution of the excited electron of the states S_{xy} and S_z relative to the hole,

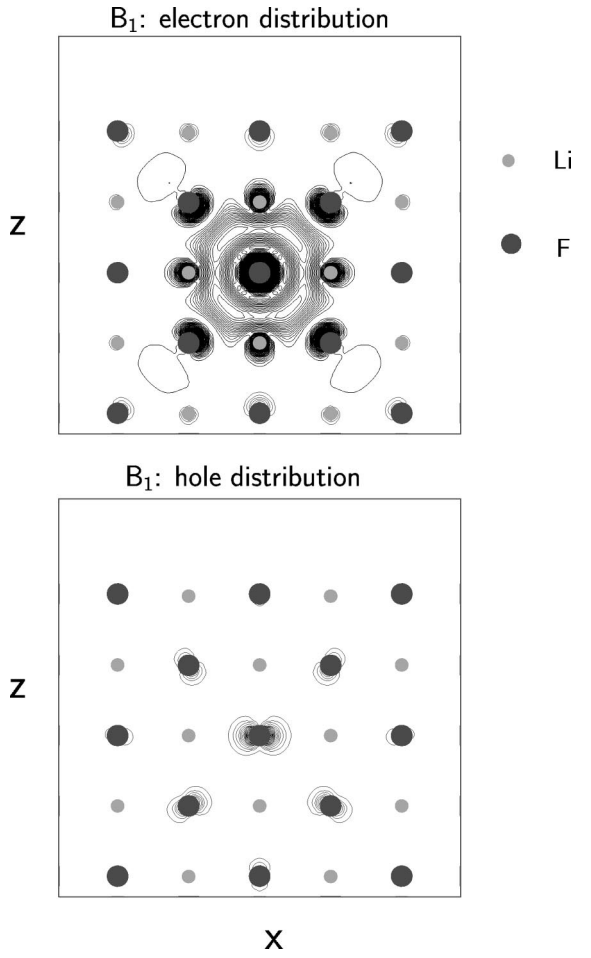

FIG. 6. Two-dimensional projections of the probability density $|\chi_S(\mathbf{r_h},\mathbf{r_e})|^2$ for the exciton state B_1 (side view). The top panel shows the distribution of the electron relative to the hole (which is fixed at a bulklike F atom in the center of the panel). The bottom panel shows the distribution of the hole relative to the electron (which is now fixed at a bulklike F atom).

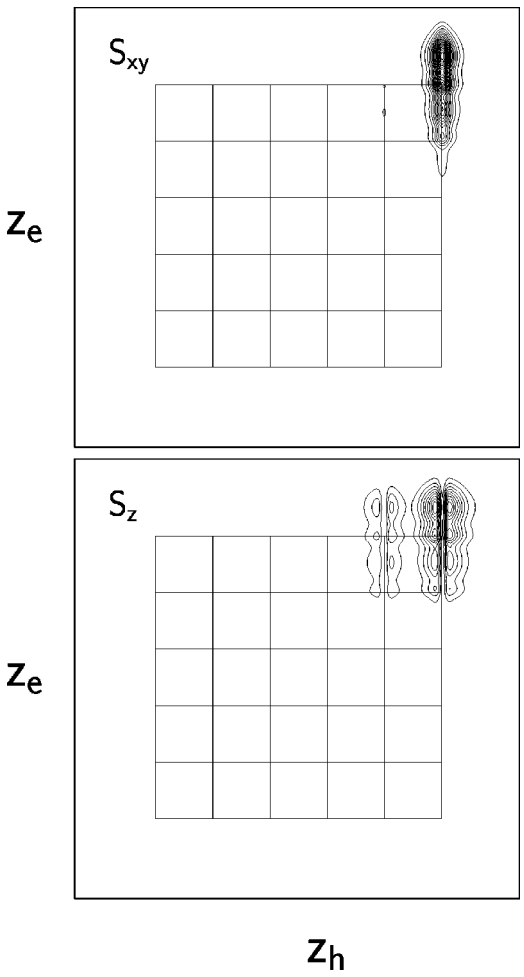

FIG. 7. Reduced z_h/z_e correlation function $\overline{\chi_S^2}$ for the two exciton states S_{xy} (top panel) and S_z (bottom panel) (cf. Fig. 5). Equivalent states occuring at the lower surface of the slab (i.e., in the lower left corner of each panel) are not explicitly shown.

which is fixed at a surface F atom. Within the atomic layers, the distributions resemble the electron distribution in the bulklike exciton (cf. the top panel of Fig. 6). In the vacuum region, however, they show significant modifications (like an overflowing muffin). In particular, the spatial extent parallel to the surface is larger than the spatial extent of the bulk exciton. Figures 8 (c) and (d) show the distribution of the *hole* relative to the electron, which is also fixed at the surface F atom. Apparently, the hole of the S_{xy} exciton state [shown in panel (c)] is mainly composed from the F $2p_x$ and $2p_y$ orbitals at the same surface F atom. The hole of the S_z state [shown in panel (d)], on the other hand, consists of the F $2p_z$ orbital at the same atom, accompanied by some contribution from F $2p_z$ states at the neighboring subsurface F atoms. This state thus extends more into the substrate than S_{xy} (cf. the discussion of Fig. 7).

In brief, the exciton states S_{xy}, B_1, and B_2 are composed of (F $2p_x/p_y \rightarrow$ Li $2s$) transitions (see again Table I). The state S_z, on the other hand, results from (F $2p_z \rightarrow$ Li $2s$) transitions. Note that p_x/p_y and p_z are no longer equivalent at the surface. This leads to the difference of 0.83 eV between the excitation energy of S_{xy} and S_z. Similar energy differences are observed between the p_x/p_y-derived bulklike states B_1 and B_2 and the corresponding p_z-derived bulklike states that are found at much higher energy (>13.5 eV).

The different orbital character of the states results in different optical properties. Simply speaking, S_{xy} and B_1 have a dipole moment in the x/y plane and are excitable by light in normal incidence. The x/y dipole moment of B_2, although being p_x/p_y related, is zero due to its nodal-structured envelope function. Therefore only the states S_{xy} and B_1 show a significant contribution to the optical spectrum at normal incidence (shown in the bottom panel of Fig. 4), which consists mainly of two peaks.

The dipole moments perpendicular to the surface, on the other hand, are zero for S_{xy}, B_1, and B_2 and nonzero for S_z. If one considers light with grazing incidence with the electric-field vector polarized along the z direction, only S_z will show a significant contribution. The resulting spectrum is shown in Fig. 9. The peaks at 12.3 and 12.8 eV (S_{xy} and B_1, respectively; cf. Fig. 4) have basically vanished and are replaced by the peak at 12.8 eV, resulting from the S_z state. Note that light with grazing incidence is associated with a

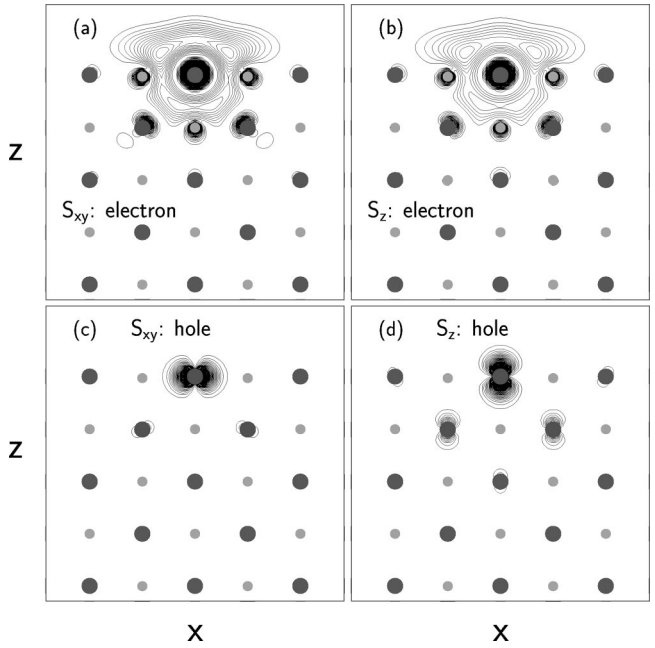

FIG. 8. Two-dimensional projections (side views) of the probability density $|\chi_S(\mathbf{r_e},\mathbf{r_h})|^2$ for the surface exciton states S_{xy} [panels (a) and (c)] and S_z [panels (b) and (d)]. Panels (a) and (b) show the distribution of the electron (relative to the hole, which is fixed at a surface F atom). Panels (c) and (d) show the distribution of the hole (relative to the electron, which is now fixed at a surface F atom).

momentum **Q** which is now *parallel* to the surface (along x in our present geometry), different from the case discussed above. This results in subtle changes in the electron-hole interaction K^{eh}, in particular in the exchange term which contains nonanalytical dipole terms. In the present case, changing **Q** from the z to the x direction results in an energy shift of S_z by 0.3 eV, yielding the modified excitation energy of 12.8 eV.

C. Optical reflectivity

The imaginary part of the dielectric response discussed in Figs. 4 and 9 corresponds to the absorption spectrum, which

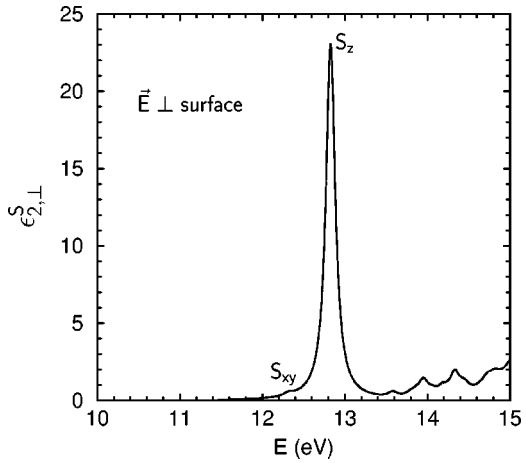

FIG. 9. Optical-absorption spectrum of the surface, calculated for grazing-incidence light (with the electric field being polarized perpendicular to the surface). The broadening is 0.07 eV.

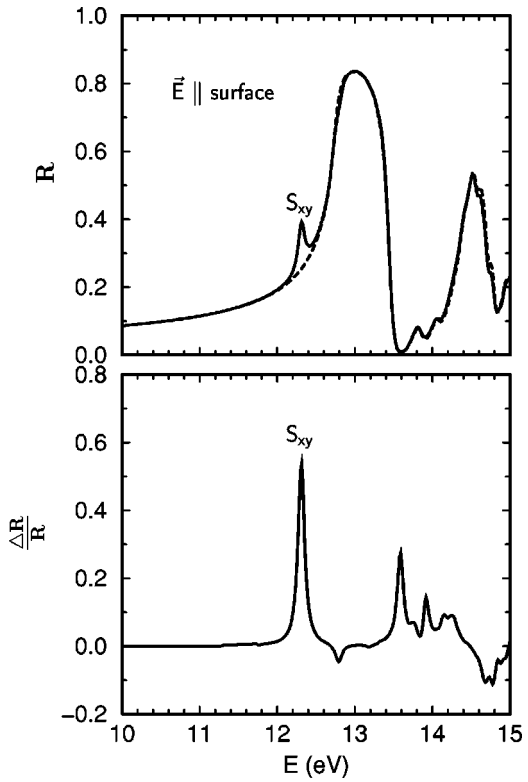

FIG. 10. Top panel: reflectivity spectrum of LiF, calculated for normal incidence. The dashed curve shows the bulk reflectivity, as obtained from the bulk dielectric function (cf. Fig. 2). The solid curve shows the reflectivity of the surface-terminated LiF crystal, including the influence of the surface (see text). The broadening is 0.05 eV. Bottom panel: relative change $\Delta R/R$ of the reflectivity due to the surface.

is very difficult to measure for a surface system. It is much easier to detect its *reflectivity* spectrum, which can also be evaluated from our bulk and surface results (shown in Fig. 10). The reflectivity of a surface system can be decomposed into two parts, i.e., a bulk reflectivity $R_{Bulk}(\omega)$ and a surface contribution $\triangle R(\omega)$. The bulk reflectivity is simply obtained from the bulk dielectric constant $\epsilon^{Bulk}(\omega)$ (cf. Fig. 2). This bulk reflectivity spectrum is shown by the dashed line in the top panel of Fig. 10. It is dominated by a broad maximum between 12.5 and 13.5 eV corresponding to the bulk exciton peak in Fig. 2. The reflectivity of the *surface*, on the other hand, is not simply given by the bulk spectrum. Instead, the reflectivity becomes modified by the electronic surface states, which shift spectral weight from bulk to surface states. For normal incidence, i.e., with the electric-field vector parallel to the surface, this change of the reflectivity is given by[32]

$$\frac{\triangle R}{R} = -\frac{8\pi d}{\lambda}\left[\frac{(1-\epsilon_1^{Bulk})(\epsilon_2^{Surf}-\epsilon_2^{Bulk})}{(1-\epsilon_1^{Bulk})^2+(\epsilon_2^{Bulk})^2} + \frac{\epsilon_2^{Bulk}(\epsilon_1^{Surf}-\epsilon_1^{Bulk})}{(1-\epsilon_1^{Bulk})^2+(\epsilon_2^{Bulk})^2}\right]. \quad (7)$$

with $\epsilon^{Surf}(\omega)$ being the optical response of the surface layer (of thickness d), as obtained from our slab calculation. The resulting reflectivity spectrum of the surface is shown by the solid line in the top panel of Fig. 10. Note that this result is a macroscopic quantity (independent of the details of the calculation, like the slab thickness), and should be directly comparable to experimental spectra.

The reflectivity of the surface is nearly identical to the bulk reflectivity, with only one characteristic difference: A small additional peak occurs at 12.3 eV, on the low-energy shoulder of the bulk-exciton peak. This small peak results from the surface exciton S_{xy}. To obtain a reasonable amplitude of this peak and separate it from the bulk background, a fairly high spectral resolution is required (0.05 eV in Fig. 10). This feature, as tiny as it may appear in Fig. 10, constitutes, in our opinion, the ultimate signature of the surface exciton at LiF(001). To our knowledge, experimental high-resolution reflectivity data of LiF(001) are not available, to date. It would be highly revealing if this feature could be detected experimentally to check the validity of our approach and our conclusions.

The bottom panel of Fig. 10 shows the relative change $\triangle R/R$ of the reflectivity due to the surface. The most prominent feature is the strong peak at 12.3 eV due to the surface exciton S_{xy}, which leads to a 50% enhancement of the reflectivity at that energy. A slightly negative value of $\triangle R/R$ is found at 12.8 eV, resulting from the reduced density-of-states of the bulklike excitons in the surface layer. Additional features are found above 13.5 eV. These structures, however, may be difficult to measure because the reflectivity itself is very small between 13.5 and 14.2 eV.

D. Comparison with experiment

In EELS spectroscopy of LiF(001), peaks are observed around 10.3 eV and around 13.5 eV, which have been interpreted as signatures of surface and bulk exciton states.[3,4] In excitation-stimulated particle desorption from LiF, an excited state at an even lower energy of 9.6 eV has been observed.[5] These data would indicate an increase of excitonic binding energy by more than 3 eV compared to the bulk. This is one order of magnitude larger than the increase of binding energy obtained in our present approach (0.4 eV). We thus conclude that our approach, which has been shown to yield reliable data for a large variety of bulk and surface systems, does not support the interpretation of the measured features at 10.3 or 9.6 eV as surface excitons of the *clean, impurity-free* LiF(001) surface. At this moment we can only speculate that the experimentally observed states may be related to more complicated features, like, e.g., point defects at the surface, surface steps, or other perturbations of the perfect LiF(001)-(1×1) surface. Another possible explanation could be that the experimental data refer to excited states of more complex nature than the excitons discussed in this paper.

VI. CONCLUSIONS

In this work we have addressed the excited electronic states of a prototype insulator surface, LiF(001)-(1×1). A recently developed *ab initio* approach is employed which solves the quantum-mechanical many-body problem step by step: based on the electronic ground state (described by density-functional theory), we calculate the single-particle excitations within the GW method and, finally, solve the Bethe-Salpeter equation for coupled electron-hole states, including the electron-hole interaction. This approach, which can be considered as the state of the art for electronic excitations, yields both bound exciton states below the fundamental gap energy, as well as the entire linear optical response above the gap.

The most salient result in the present situation of an insulator surface is the occurrence of strongly bound surface excitons with binding energies that are significantly stronger than those of LiF bulk excitons. Our approach has allowed to obtain detailed insight into the properties of these states, like their wave function, orbital composition, and spatial localization. Such excited surface states, as fascinating as they are, are difficult to directly observe in experiment. The most promising quantity to be detected in measurements is a small but distinct additional peak in the surface reflectivity, 0.4 eV below the strong structure corresponding to the bulk exciton.

Our calculated transition energies, that have been obtained for the clean, perfectly ordered LiF(001) surface, are 2 to 3 eV higher in energy than the excitations measured in electron energy-loss spectroscopy or excitation-stimulated particle desorption. A possible explanation could be that the experimental spectra may exhibit states related to defects. If this is the case, a final conclusion on the nature of these states would only be possible after calculating the excited states at imperfect surfaces.

ACKNOWLEDGMENTS

We thank A. Mazur for useful discussions. This work was financially supported by the Deutsche Forschungsgemeinschaft (Bonn, Germany) under Grant Nos. Ro 1318/4-1 and Ro 1318/5-1.

*On leave from Fudan University, Shanghai, People's Republic of China.

[1] P. Chiaradia, A. Cricenti, S. Selci, and G. Chiarotti, Phys. Rev. Lett. **52**, 1145 (1984); M.A. Olmstead and N.M. Amer, *ibid.* **52**, 1148 (1984); F. Ciccacci, S. Selci, G. Chiarotti, and P. Chiaradia, *ibid.* **56**, 2411 (1986); B.S. Mendoza, R. Del Sole, and A.I. Shkrebtii, Phys. Rev. B **57**, R12 709 (1998).

[2] Y. Harada, J.N. Murrell, and H.H. Sheena, Chem. Phys. Lett. **1**, 595 (1968); M. Suto and L.C. Lee, J. Chem. Phys. **84**, 1160 (1986); C. Goletti, F. Arciprete, S. Almaviva, P. Chiaradia, N. Esser, and W. Richter, Phys. Rev. B **64**, 193301 (2001).

[3] G. Roy, G. Singh, and T.E. Gallon, Surf. Sci. **152/153**, 1042

(1985); T.E. Gallon, *ibid.* **206**, 365 (1988).
[4] T. Mabuchi, J. Phys. Soc. Jpn. **57**, 241 (1988).
[5] P. Wurz *et al.*, Phys. Rev. B **43**, 6729 (1991).
[6] H. Tatewaki and E. Miyoshi, Surf. Sci. **327**, 129 (1995).
[7] H. Winter *et al.*, J. Phys. B **35**, 3315 (2002).
[8] M.S. Hybertsen and S.G. Louie, Phys. Rev. Lett. **55**, 1418 (1985); **34**, 5390 (1986).
[9] W. Hanke and L.J. Sham, Phys. Rev. B **21**, 4656 (1980).
[10] G. Onida, L. Reining, R.W. Godby, R. Del Sole, and W. Andreoni, Phys. Rev. Lett. **75**, 818 (1995); S. Albrecht, L. Reining, R. Del Sole, and G. Onida, *ibid.* **80**, 4510 (1998).
[11] L.X. Benedict, E.L. Shirley, and R.B. Bohn, Phys. Rev. Lett. **80**, 4514 (1998); Phys. Rev. B **57**, R9385 (1998).
[12] M. Rohlfing and S. G. Louie, Phys. Rev. Lett. **80**, 3320 (1998); **81**, 2312 (1998); **82**, 1959 (1999); **83**, 856 (1999).
[13] M. Rohlfing and S.G. Louie, Phys. Rev. B **62**, 4927 (2000).
[14] L. Hedin, Phys. Rev. **139**, A796 (1965).
[15] L. Hedin and S. Lundqvist, in *Solid State Physics, Advances in Research and Application*, edited by F. Seitz, D. Turnbull, and H. Ehrenreich (Academic, New York, 1969), Vol. 23, p. 1.
[16] G. Strinati, Phys. Rev. Lett. **49**, 1519 (1982): Phys. Rev. B **29**, 5718 (1984).
[17] M. Rohlfing, Appl. Phys. A: Mater. Sci. Process. **72A**, 413 (2001).
[18] M. Rohlfing and S.G. Louie, Phys. Status Solidi A **175**, 17 (1999); M. Rohlfing, M. Palummo, G. Onida, and R. Del Sole, Phys. Rev. Lett. **85**, 5440 (2000).
[19] P.H. Hahn, W.G. Schmidt, and F. Bechstedt, Phys. Rev. Lett. **88**, 016402 (2002).
[20] M. Rohlfing, P. Krüger, and J. Pollmann, Phys. Rev. B **48**, 17 791 (1993); **52**, 1905 (1995).
[21] G.B. Bachelet, D.R. Hamann, and M. Schlüter, Phys. Rev. B **26**, 4199 (1982).
[22] M.S. Hybertsen and S.G. Louie, Phys. Rev. B **37**, 2733 (1988).
[23] F.J. Himpsel *et al.*, Phys. Rev. Lett. **68**, 3611 (1992).
[24] E.L. Shirley, L.J. Terinello, J.E. Klepeis, and F.J. Himpsel, Phys. Rev. B **53**, 10 296 (1996).
[25] L.I. Johansson and S.B.M. Hagström, Phys. Scr. **14**, 55 (1976).
[26] S.P. Kowalczyk *et al.*, Phys. Rev. B **9**, 3573 (1974).
[27] D.M. Roessler and W.C. Walker, J. Opt. Soc. Am. **57**, 835 (1967).
[28] G.C. Benson and T.A. Claxton, J. Chem. Phys. **48**, 1356 (1968); T.E. Gallon, I.G. Higginbotham, M. Prutton, and H. Tokutaka, Surf. Sci. **21**, 224 (1970); G.E. Laramore and A.C. Switendick, Phys. Rev. B **7**, 3615 (1973); M.R. Welton-Cook and W. Berndt, J. Phys. C **15**, 5691 (1982); S. Pugh and M.J. Gillan, Surf. Sci. **320**, 331 (1994).
[29] The relaxations have been calculated for the surface with the optimized theoretical lattice constant of 3.918 Å and have then been scaled to the experimental lattice constant of 4.026 Å. The resulting relaxations are then used for the calculation of the spectra.
[30] J. Vogt and H. Weiss, Surf. Sci. **501**, 203 (2002).
[31] The fourfold degeneracy of S_{xy} results from the equivalence of the F $2p_x$ and $2p_y$ orbitals from which the transition originates, and from the equivalence of the two surfaces of the slab. The twofold degeneracy of B_1 (and also of B_2) results from the equivalence of F $2p_x$ and $2p_y$; the twofold degeneracy of S_z results from the equivalence of the two surfaces. The degeneracy (which is better than 0.02 eV in our results) of the four S_{xy} states (and of the two S_z states) indicates that there is no overlap of the surface states of the upper and lower surface, i.e., that the six-layer slab is sufficiently thick to decouple the two surfaces.
[32] S. Selci, F. Ciccacci, G. Chiarotti, P. Chiaradia, and A. Cricenti, J. Vac. Sci. Technol. A **5**, 327 (1987).